Electronic Supplementary Material (ESI) for Journal of Materials Chemistry A.

Electronic Supporting Information

Understanding the Stability of Mixed A-Cation Lead Iodide Perovskites

B. Charles, J. Dillon, O. J. Weber, M. S. Islam and M. T Weller

S1 Experimental

Formamidinium iodide was purchased from Dysol, with all other reagents purchased from Sigma Aldrich. Solvents were purchased from Alfa Aesar with purities > 99%.

Precursor synthesis of methylammonium iodide (MAI) was carried out. 16.620ml of hydroiodic acid (57 wt %) was stabilised using 1.5 wt % H_3PO_2 and then added dropwise to 10.891ml of methylamine (40 wt % in H_2O) in an ice bath under stirring. After 1 hour the H_2O was removed through rotary evaporation. The resulting MAI was then recrystallised using ethanol and oven dried overnight.

Thin film deposition of $MA_{1-x}FA_xPbI_3$ perovskites was achieved through spin coating on clean glass substrates. The glass substrates were cleaned sequentially using liquid detergent, acetone and ethanol in an ultrasonic bath for 10 minutes. MAI and FAI were weighed such that the MAI:FAI ratio varied from 1 to 0 in increments of 0.1 before being dissolved with PbI_2 in DMF (0.6 molar). 100 µL of the resulting solutions were deposited onto the clean glass substrates under a dry atmosphere and spin coated at 4000 rpm for 30 s. The films were then transferred to a hot plate and annealed at 110 °C for 30 minutes.

Powder X-ray diffraction was used to characterise the $MA_{1-x}FA_xPbI_3$ thin films. A Bruker Advance D8 X-ray diffractometer with a Cu-Kα radiation was used. The diffraction angle was scanned from 10 ° to 50 ° using a step size of 0.016 °.

Scanning electron microscopy (SEM) images were taken of $MA_{1-x}FA_xPbI_3$ (x = 0.3, 0.5, 0.6, 0.7) using a Jeol JSM-6480LV SEM. Secondary electron images of the films were taken using an accelerating voltage of 5KV at magnifications of x500, x1000 and x2500.

Ab initio simulation techniques based on density functional theory (DFT) (employing the code VASP58 code) were used to examine the energetics of the mixed $MA_{1-x}FA_xPbI_3$ system. A cell of XXX atoms of the pseudo-cubic unit cells were modelled; a plane wave cut off energy of 520 eV, *k*-point sampling at the gamma point, PAW pseudopotentials and a GGA+VdW (OptB86b) exchange-correlation functional were employed. For structure relaxation, forces were converged to less than 0.01 eV/Å-1. The simulations reproduce the experimental crystal structures of MAPI and FAPI in good agreement with diffraction data.[9,12]

S2 – X-Ray Diffraction Patterns

X-ray diffraction patterns of thin films $MA_{1-x}FA_xPbI_3$. The presence of PbI_2 was characterised through the presence of the (001) reflection centered at 2θ = 12.7°. Formation of PbI_2 is suppressed with increasing FA content, until x = 0.6, where only trace amounts of PbI_2 are observed after 10 days. Multiple films of x = 0.6 were synthesised, of which one repeat is shown in Fig.S2.1. It was observed that even trace amounts of PbI_2 present in as-made films caused rapid degradation of the films (See S3 for kinetic analysis). Therefore is was concluded that pristine, phase pure perovskite films are required to prevent degradation into PbI_2 and precursor salts.

For compositions where $x \geq 0.7$ the hexagonal δ-FAPI peak is observed immediately after deposition. Formation of the δ-phase is supressed at x = 0.7 due to MA; however this is overcome as $x \geq 0.8$ where the intensity of the δ-phase peak surpasses the strongest perovskite reflection, the (100) peak centred around 2θ = 14°. Films of $x \geq 0.8$ were seen to transform into the yellow δ-phase within minutes of exposure to air.

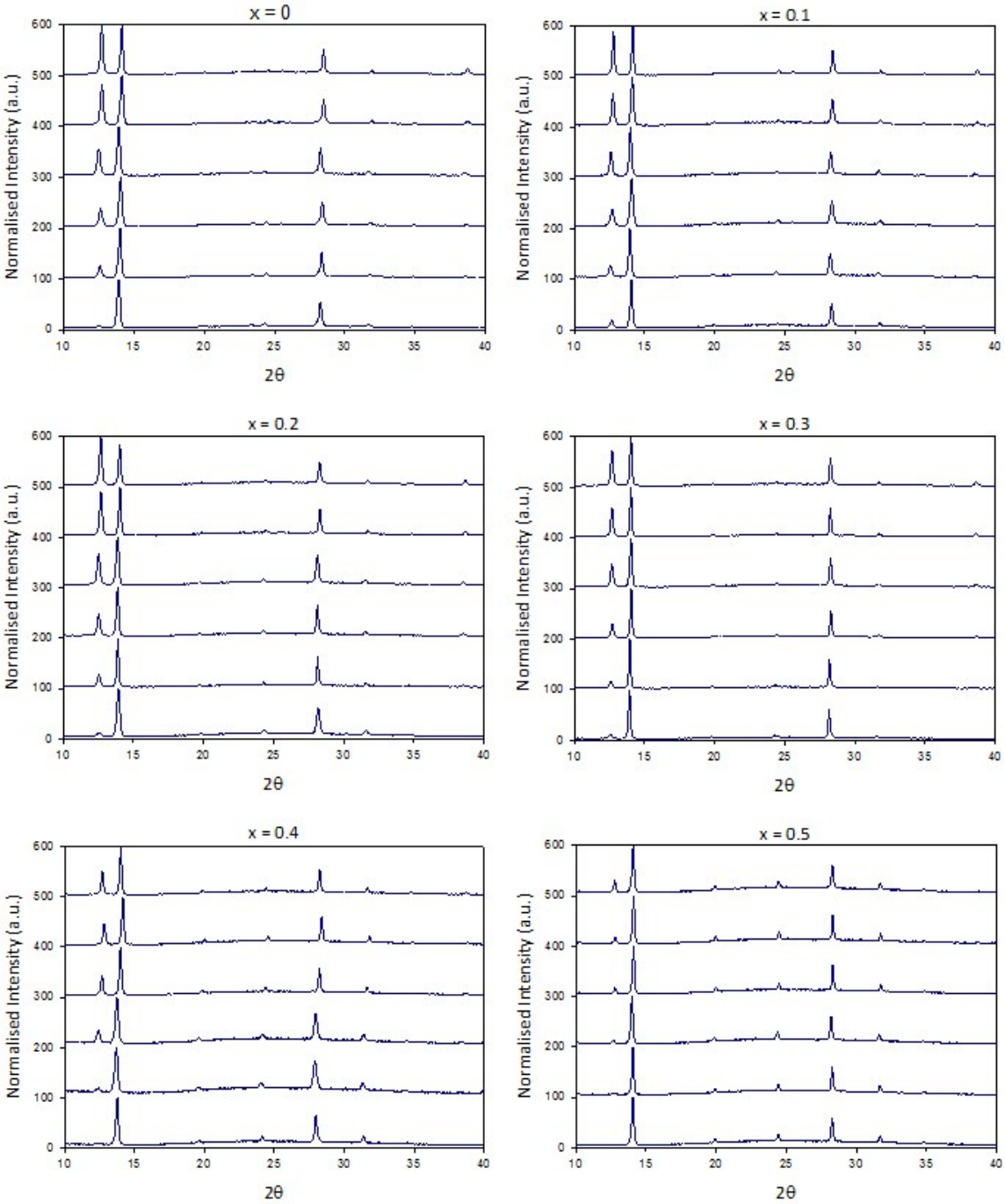
x = 0
x = 0.1
x = 0.2
x = 0.3
x = 0.4
x = 0.5
Normalised Intensity (a.u.)
2θ
0
100
200
300
400
500
600
10
15
20
25
30
35
40

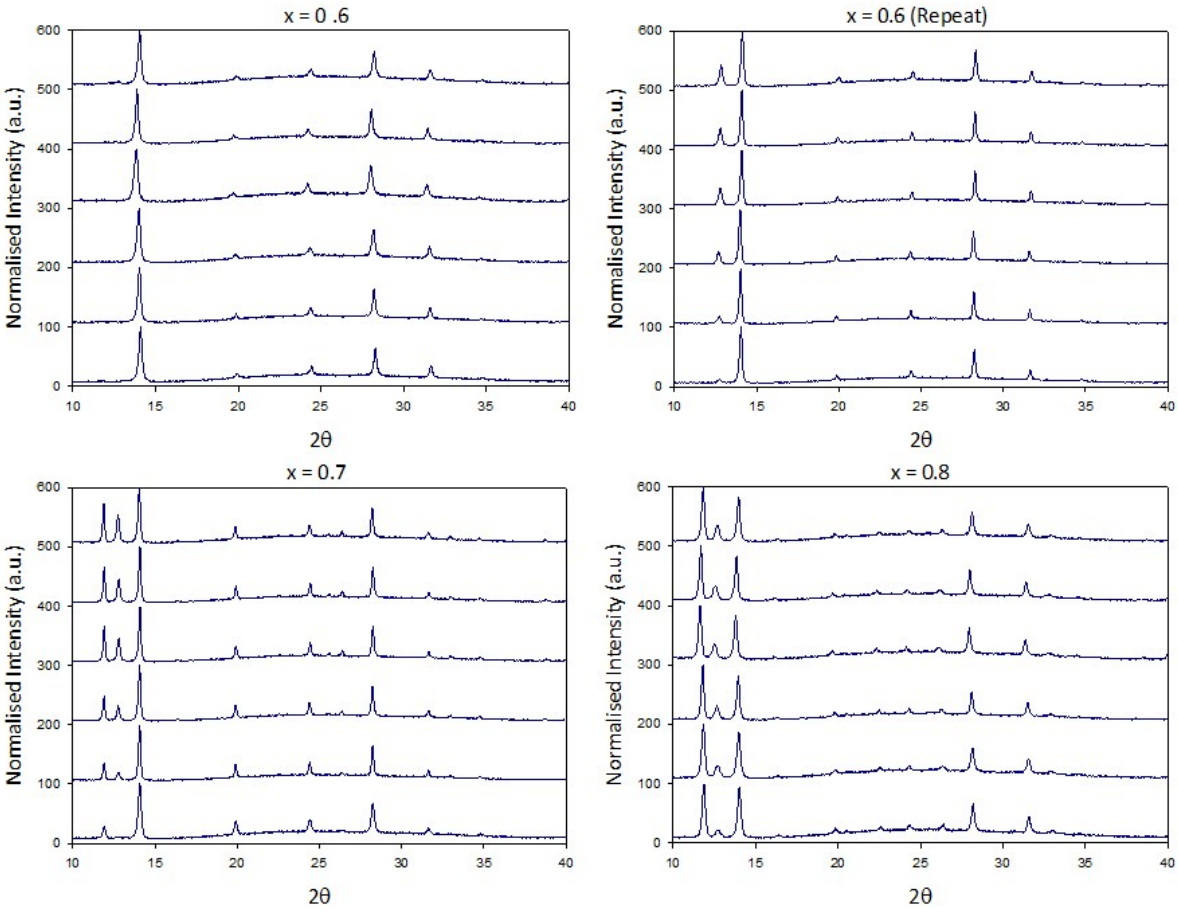

Fig.S2.1 X-ray Diffraction patterns of the $MA_{1-x}FA_xPbI_3$, $0 \leq x \leq 0.8$, thin films. Patterns were measured immediately after synthesis (bottom trace) and then through 1, 3, 5, 7 and 10 days (top trace).

S3 – Kinetic Analysis of $MA_{0.4}FA_{0.6}PbI_3$ and $MA_{0.3}FA_{0.7}PbI_3$

The Johnson-Mehl-Avrami-Kolmogorov (JMAK, equation 1) was used to model the crystallisation of PbI_2 in the thin films of $MA_{1-x}FA_xPbI_3$, $0 \leq x \leq 0.6$. In which the phase fraction of PbI_2 present was approximated through the peak area of the (001) PbI_2 reflection in PXD patterns.

It was observed that for phase pure $MA_{0.4}FA_{0.6}PbI_3$ only trace amounts of PbI_2 were present after 10 days stored under air in the dark. However, the presence of PbI_2 in as made films caused rapid degradation. Fig.S3.1 shows three repeats of the 10 day degradation study for $x = 0.6$ films. Each as made film contained small quantities of PbI_2 which accelerated degradation, however the rate of this decomposition remained lower than the MA-rich phases. The more PbI_2 present in the as made films the faster the initial decomposition.

PbI_2 was not modelled this way for $x \geq 0.7$ due to the competing degradation pathway to the δ-FAPI phase. However the kinetics of formation of the δ-FAPI phase was briefly investigated and also found to follow the JMAK model, using the peak area under the δ-FAPI reflection centred around $2\vartheta = 11.7°$ as an approximation for phase fraction.

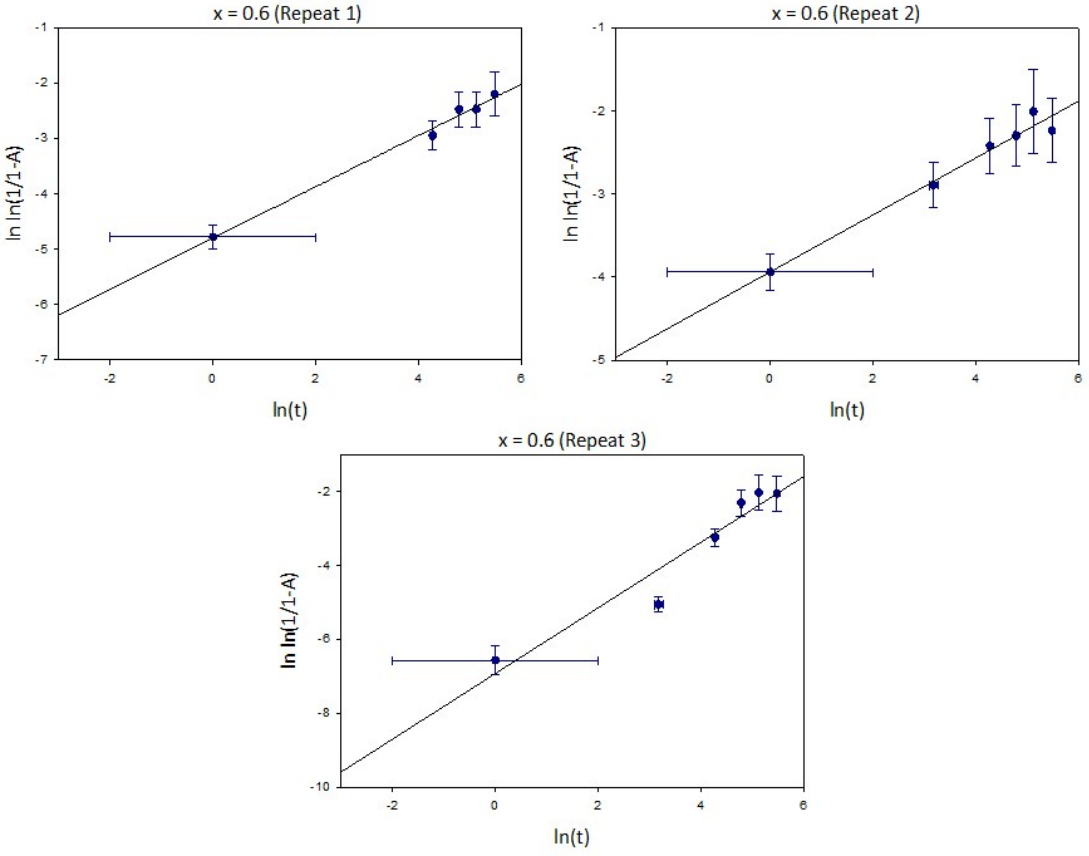

Fig.S3.1 Kinetic plots for the growth of PbI_2 in $MA_{0.4}FA_{0.6}PbI_3$ where t is time in hours and A the peak area of the (001) PbI_2 reflection. As made films contained small quantities of PbI_2 accelerating film decomposition.

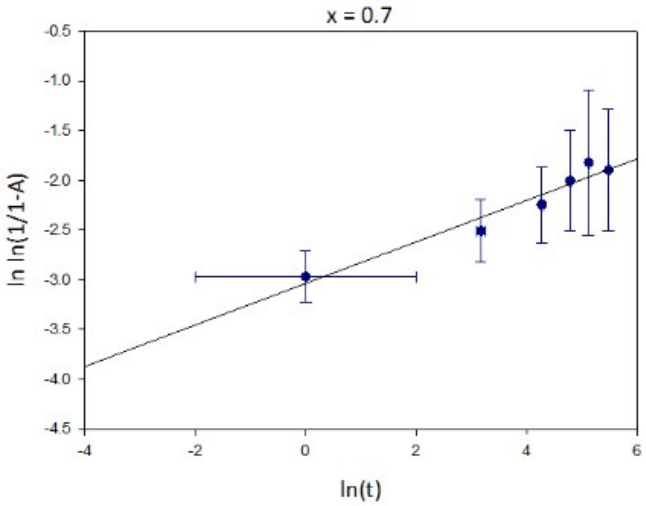

Fig.S3.1 Kinetic plot for the growth of the δ-FAPI phase in $MA_{0.3}FA_{0.7}PbI_3$ where *t* is time in hours and *A* the peak area of the δ-FAPI reflection centred around 2θ = 11.7°. The linear relationship observed suggests the kinetics of δ-FAPI formation also follows the JMAK model.

S4 – Decomposition Energies

The degradation energies (ΔE_{deg}) for the pathways shown in Fig. 4 were calculated for $MA_{1-x}FA_xPbI_3$ in the full composition range $0 < x < 1$. In this case:

$$Reaction\ 1\text{: } MA_{1-x}FA_xPbI_3 \rightarrow (1-x)MAI + xFAI + PbI_2$$

$$Reaction\ 2\text{: } MA_{1-x}FA_xPbI_3 \rightarrow (1-x)(MAI + PbI_2) + x(\delta - FAPbI_3).$$

Alternate starting conditions were assumed on either the cubic, high order or low order structure of FAPI, the tetragonal structure of MAPI or a large disordered cell consisting of 64 formula units. MA and FA were then substituted into these cells in the desired ratios. ΔE_{deg} was plotted against $MA_{1-x}FA_xPbI_3$ for each of the different starting conditions (Fig. S4.1).

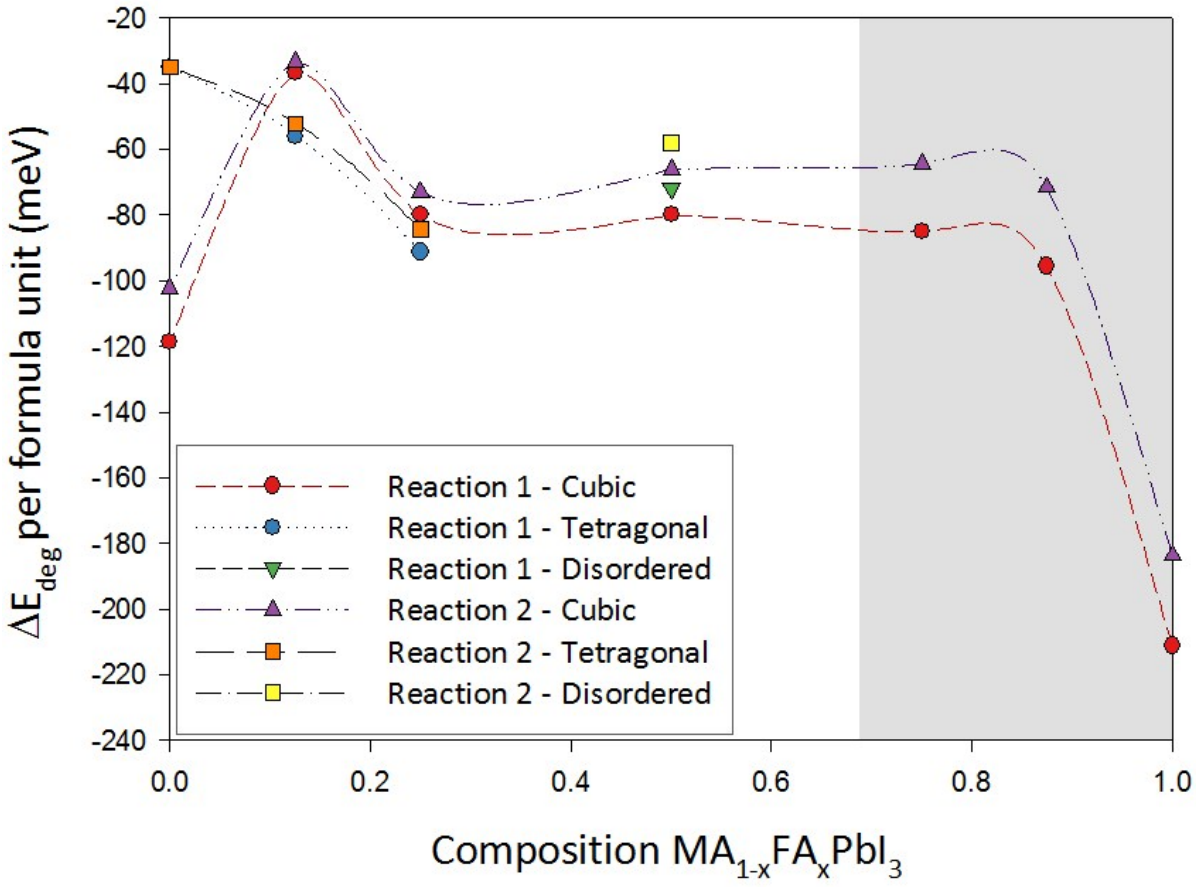

Fig.S4.1 Calculated energies for the decomposition reaction 1 and 2 for $MA_{1-x}FA_xPbI_3$. The dotted lines act as a guide to the eye.

S5 – Film Morphology

Scanning electron microscopy (SEM) was used to obtain images of thin films of $MA_{1-x}FA_xPbI_3$ (x = 0.3, 0.5, 0.6, 0.7) to compare differences in film morphology. Crystallite size was measured to increase from an average of 3µm to 3.5µm for x = 0.3 and 0.6 respectively. However a doubling to 6µm was observed in x = 0.7 films, coinciding with the presence of the hexagonal (non-perovskite) δ-phase. The small variation in crystallite size for x < 0.7 was judged not to significantly affect film degradation.

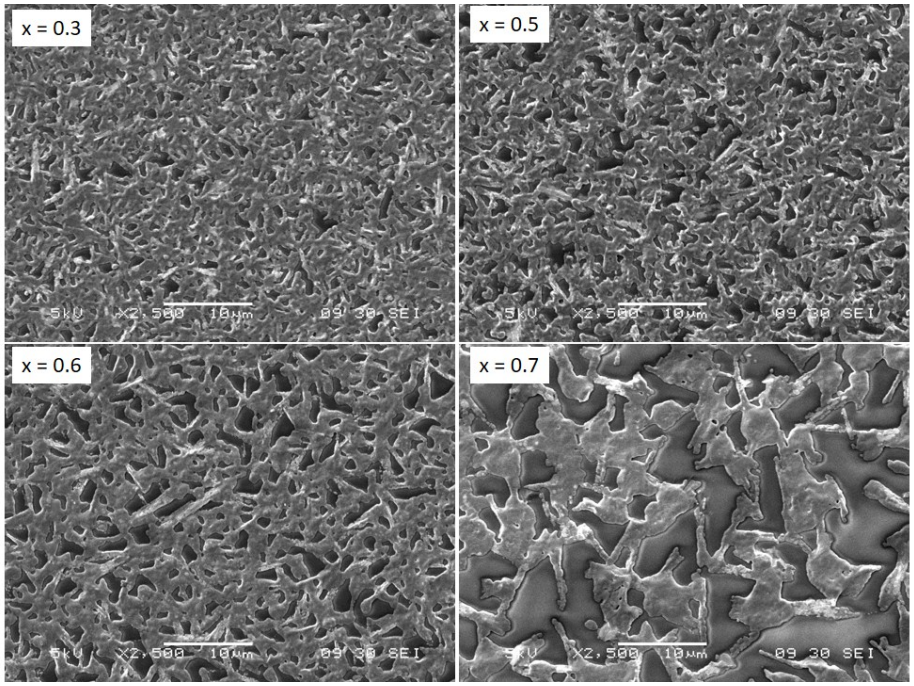

Fig.S5.1 SEM images $MA_{1-x}FA_xPbI_3$ (x = 0.3, 0.5, 0.6, 0.7) thin films taken at a magnification of x2500

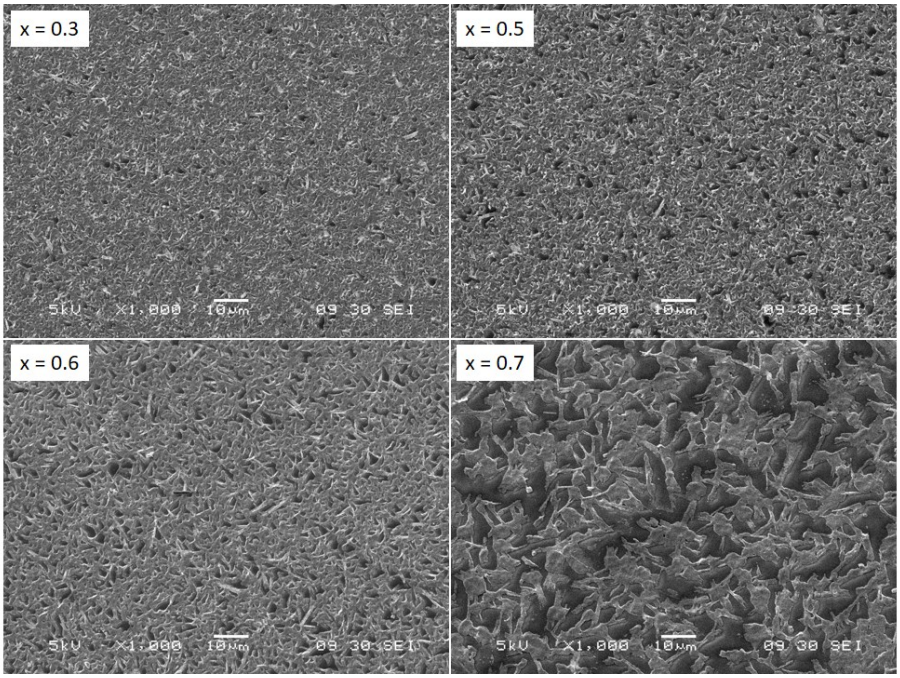

Fig.S5.2 SEM images $MA_{1-x}FA_xPbI_3$ (x = 0.3, 0.5, 0.6, 0.7) thin films taken at a magnification of x1000

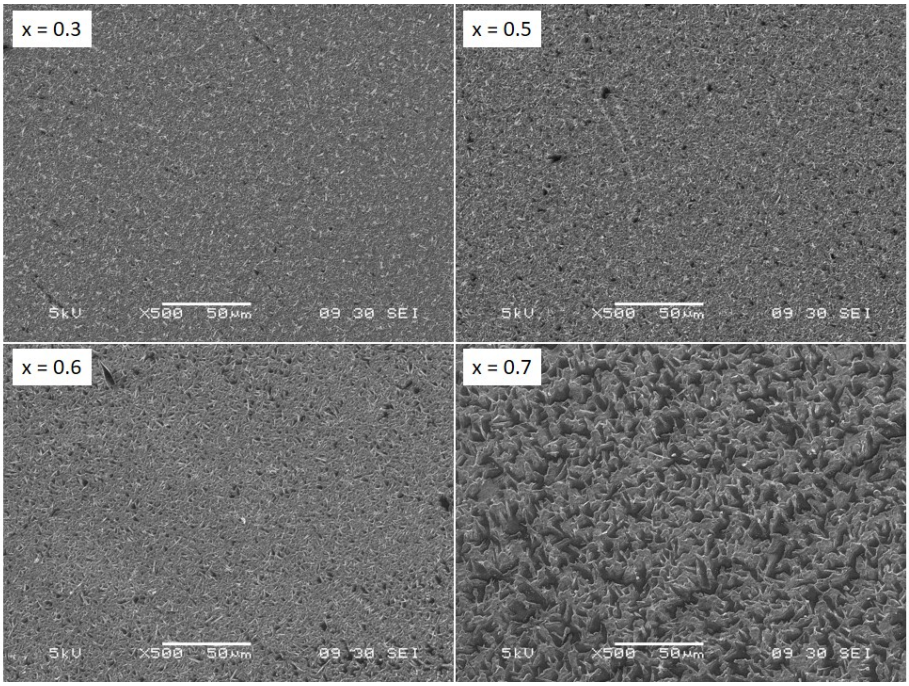

Fig.S5.3 SEM images $MA_{1-x}FA_xPbI_3$ (x = 0.3, 0.5, 0.6, 0.7) thin films taken at a magnification of x500